

NGDB-Zoo: Towards Efficient and Scalable Neural Graph Databases Training

Zhongwei XIE¹ Jiaxin BAI¹ Shujie LIU² Haoyu HUANG¹ Yufei LI¹ Yisen GAO¹ Hong Ting TSANG¹
Yangqiu SONG¹

Abstract

Neural Graph Databases (NGDBs) facilitate complex logical reasoning over incomplete knowledge structures, yet their training efficiency and expressivity are constrained by rigid query-level batching and structure-exclusive embeddings. We present **NGDB-Zoo**, a unified framework that resolves these bottlenecks by synergizing **operator-level training** with **semantic augmentation**. By decoupling logical operators from query topologies, NGDB-Zoo transforms the training loop into a dynamically scheduled data-flow execution, enabling multi-stream parallelism and achieving a $1.8\times - 6.8\times$ throughput compared to baselines. Furthermore, we formalize a decoupled architecture to integrate high-dimensional semantic priors from Pre-trained Text Encoders (PTEs) without triggering I/O stalls or memory overflows. Extensive evaluations on six benchmarks, including massive graphs like *ogbl-wikikg2* and *ATLAS-Wiki*, demonstrate that NGDB-Zoo maintains high GPU utilization across diverse logical patterns and significantly mitigates representation friction in hybrid neuro-symbolic reasoning.

1. Introduction

Neural Graph Databases (NGDBs) have emerged as a powerful paradigm for complex logical reasoning over large-scale, incomplete knowledge structures (Ren et al., 2023; Besta et al., 2022; Shi et al., 2025; Pengmei et al., 2024). By embedding existential first-order logic queries into continuous geometric spaces, these systems enable approximate retrieval and inductive inference beyond symbolic traversal (Ren et al., 2020; Bai et al., 2023). Despite their promise, the transition from theoretical models to production-ready query engines is hindered by a fundamental tension between **hardware efficiency** and **representational expressivity**.

¹The Hong Kong University of Science and Technology

²Microsoft Research Asia. Correspondence to: Yangqiu SONG <yqsong@cse.ust.hk>.

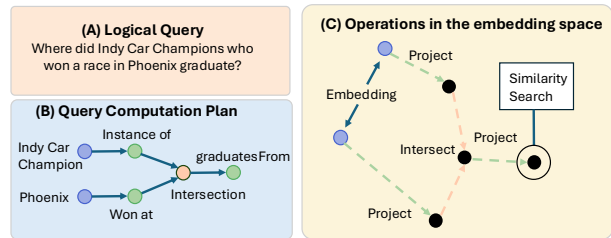


Figure 1. **Task Illustration.** Query embedding methods aim to answer multihop logical queries (A) by avoiding explicit knowledge graph traversal and executing the query directly in the embedding space by following the query computation plan (B). Operators are executed in the embedding space (C).

We identify two prohibitive challenges that prevent the realization of scalable NGDBs: **First, Computational Efficiency and Topological Rigidity.** Existing dense-retrieval-based training frameworks rely on batching at the query level, which constrains a single mini-batch to queries sharing isomorphic logical structures (e.g., 2i) (Ren & Leskovec, 2020; Ramezanpour et al., 2025; Zeng et al., 2024). This constraint causes severe hardware under-utilization when processing diverse query mixtures, as kernels are fragmented by the high entropy of real-world query workloads. As link density drops in large-scale graphs, this efficiency bottleneck becomes a barrier to convergence. **Second, Representation Friction in Hybrid Integration.** While treating entities as atomic tokens is sufficient for dense Knowledge Graphs, NGDBs require richer semantic units to perform robust reasoning in sparse or inductive settings. Augmenting structural embeddings with high-dimensional semantic priors (e.g., from Pretrained Language Models) can compensate for graph sparsity (Wei et al., 2025; Wang et al., 2021b; Kim et al., 2022; Chen et al., 2025b; Feng et al., 2025; Tang et al., 2024), however it introduces significant system-level friction. The integration of large semantic vectors often triggers I/O stalls and memory overflows during multi-processing, creating a trade-off where representational gains are offset by catastrophic training latency.

To resolve these challenges, we present **NGDB-Zoo**, a unified framework designed for high-throughput and semantically-aware neural graph reasoning. Our approach decouples logical operators from fixed query topologies, transforming the training loop into a dynamically scheduled

data-flow execution. Our contributions are as follows:

Contribution 1: Operator-Level Training Paradigm. We propose a novel training paradigm that shifts the batching granularity from query-level isomorphism to operator-level batching. By decomposing complex queries into a Directed Acyclic Graph (DAG) of operators, this enables dynamic scheduling and cross-query operator fusion, achieving a SOTA training throughput over standard baselines.

Contribution 2: Decoupled Semantic Integration Architecture. We develop a modal-agnostic framework to fuse structural embeddings with high-dimensional external signals from Pretrained Text Encoders (PTEs). To mitigate system bottlenecks, we implement decoupled semantic encoding and high-throughput GPU-Resident integration, enabling the efficient handling of semantic parameters without I/O blocking.

Contribution 3: Scalable Neuro-Symbolic Benchmarking. We provide a rigorous evaluation across six benchmarks, including massive graphs like *ogbl-wikikg2* and *ATLAS-Wiki*. Experimental results demonstrate that NGDB-Zoo achieves a $1.8\times$ – $6.8\times$ increase in training throughput compared to state-of-the-art baselines. Our analysis characterizes the efficiency-expressivity trade-off in hybrid models and offers a technical roadmap for handling non-stationary query distributions through adaptive online sampling.

2. Related Work

Neural Graph Databases Reasoning. Complex Query Answering (CQA) extends relational link prediction to multi-hop logical operations. Early methods (Yang et al., 2014; Trouillon et al., 2016) focused on simple relational patterns. More recent geometric embedding models (Xiong et al., 2023) represent queries as points (Sun et al., 2019), bounded regions (Ren et al., 2020; Zhang et al., 2021; Wu et al., 2024), or probabilistic distributions (Ren & Leskovec, 2020; Yang et al., 2022) to capture topological constraints and uncertainty. Complementary approaches utilize hyperbolic projections (Choudhary et al., 2021) or sequential encoding (Bai et al., 2023). Recently, standalone models have evolved into integrated Neural Graph Databases (NGDBs) (Besta et al., 2022; Ren et al., 2023; Hu et al., 2024b;a; Zheng et al., 2025; Wang et al., 2025; Choi et al., 2025), supporting neuro-symbolic retrieval at scale and providing the state-space foundation for autonomous planning in Agentic NGDBs (Bai et al., 2025b; Lefebvre & Varoquaux, 2025). Despite their promise, the infinite, structurally diverse query space in NGDBs renders traditional offline training prohibitive, necessitating the high-throughput online sampling and operator-level optimization proposed in this work.

Training Optimization for Graph Embedding Models. Graph Neural Networks (Wu et al., 2020; Galkin et al., 2020; He et al., 2025; Finder et al., 2025; Li et al., 2025; Bao et al.,

2025) use neighbor sampling or subgraph batching. Sequence Models (Ott et al., 2019; Yan et al., 2021) batch sequences with similar lengths, padding when necessary. Knowledge Graph Embeddings (Ren et al., 2022; Ge et al., 2024; Cui et al., 2025) batch simple link prediction triples. Prior work has explored operator-level parallelism in different contexts. Compiler Optimization (Chen et al., 2023) batches operators in computational graphs for inference. Data Flow Architectures (Veen, 1986) schedule operations based on data availability. Atom (Zhou et al., 2024) introduced operator-level batching to optimize throughput in KG serving and inference systems. To the best of our knowledge, NGDB-Zoo is the first to apply operator-level batching to the training of knowledge graph embedding models.

Pretrained Embeddings for Structured Knowledge. Besides dense-retrieval-based method, recent work has explored combining pretrained language models with knowledge graphs (Ketata et al., 2025; Yao et al., 2019): KEPLER (Wang et al., 2021b) leverages KG embeddings as supervision signals to train language models. SimKGC (Wang et al., 2022) uses contrastive learning to align entity descriptions with KG structure. Some works (Galkin et al., 2023; 2024; Yun et al., 2019; Min et al., 2022; Hu et al., 2020b; Rong et al., 2020; Chen et al., 2022a; 2025a; Kim et al., 2024) build pre-trained GNN foundation model for reasoning tasks on KGs. Recent state-of-the-art encoders (Wang et al., 2021a) like Qwen3-Embedding (Zhang et al., 2025) and BGE-Embedding (Xiao et al., 2023) provide rich semantic similarity signals. However, integrating high-dimensional PLM outputs into complex multi-hop reasoning often triggers severe I/O stalls and memory bottlenecks. Fusing these semantic representations with multi-hop reasoning models efficiently remains an open challenge.

3. Problem Formulation

3.1. Complex Logical Queries

Let $\mathcal{G} = (\mathcal{E}, \mathcal{R}, \mathcal{T})$ be a knowledge graph, where \mathcal{E} is the set of entities, \mathcal{R} is the set of relations, and $\mathcal{T} \subseteq \mathcal{E} \times \mathcal{R} \times \mathcal{E}$ represents the observed fact triples. We consider the task of answering complex logical queries q that can be expressed in Existential First-Order (EFO) logic, following the form:

$$q[V_?] = \exists V_1, V_2, \dots, V_k : \phi(V_?, V_1, \dots, V_k) \quad (1)$$

where $V_?$ is the target variable (the answer), $\{V_1, \dots, V_k\}$ are existentially quantified bound variables, and ϕ is a conjunction or disjunction of atomic formulas (literals) such as (V_a, r, V_b) .

Neural Graph Databases (NGDBs) execute complex logical queries over these structures. We evaluate 14 distinct query patterns involving projection (p), intersection (i), union (u), and negation (n). These patterns ($1p, 2p, 3p, 2i, 3i, pi, ip,$

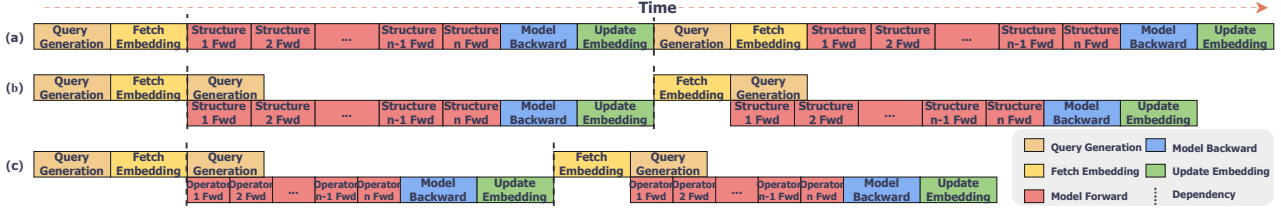


Figure 2. **Evolution toward High-Throughput Asynchronous Pipelining.** Training methods. (a) represents the naive training scheme; (b) shows the pre-sampling and pre-fetching optimization; (c) NGDB-Zoo’s operator-level approach breaks these constraints to enable fully overlapping stages, creating a dense execution stream that maximizes hardware saturation.

$2u, up, 2in, 3in, pin, pni, inp$) represent different topological constraints in the reasoning subgraph, challenging the model to perform multi-hop compositional reasoning.

3.2. The Task: Predictive Query Answering

Unlike standard database queries that rely on a complete \mathcal{G} , the **Predictive Query Answering** task requires identifying answers from an incomplete graph where many true triples are missing during the training and inference time.

Answer Set. For a given query q , we define its *denotation set* $\mathcal{A}_q \subseteq \mathcal{E}$ as the complete set of entities satisfying the logical constraints of q under the ground-truth graph \mathcal{G}_{full} . While our framework optimizes a unified objective over \mathcal{A}_q , this set is implicitly comprised of two conceptually distinct categories: *Direct Answers* (\mathcal{A}_q^{obs}), which are reachable via symbolic execution on the observed training graph \mathcal{G}_{train} , and *Predictive Answers* ($\mathcal{A}_q^{miss} = \mathcal{A}_q \setminus \mathcal{A}_q^{obs}$), which are valid under \mathcal{G}_{full} but remain latent in \mathcal{G}_{train} due to missing triples. This implicit distinction allows us to evaluate the framework’s capacity to generalize from observed relational patterns to inductive reasoning over missing knowledge.

Objective Function. The objective is to learn a scoring function $f : \mathcal{Q} \times \mathcal{E} \rightarrow \mathbb{R}$, where \mathcal{Q} is the query space. For each $e \in \mathcal{E}$, $f(q, e)$ measures the likelihood that e is a valid answer to q . The task is formulated as a ranking problem:

$$\forall e \in \mathcal{A}_q, e' \notin \mathcal{A}_q \implies f(q, e) > f(q, e') \quad (2)$$

The model must generalize beyond memorized paths by embedding the query into a latent representation $\mathbf{q} \in \mathcal{H}_{joint}$ (as defined in Section E) and computing its proximity to entity embeddings \mathbf{x}_i in the joint semantic-structural space.

Joint Structural-Semantic Representation. We define a joint representation setting where the entity embedding space is a composite manifold $\mathcal{H}_{joint} = \mathcal{H}_{str} \times \mathcal{H}_{sem}$. The structural subspace $\mathcal{H}_{str} \subseteq \mathbb{R}^{d_s}$ captures endogenous graph topology through trainable embeddings \mathbf{h}_i , while the semantic subspace $\mathcal{H}_{sem} \subseteq \mathbb{R}^{d_m}$ encapsulates exogenous linguistic priors via a frozen Pre-trained Text Encoder (PTE),

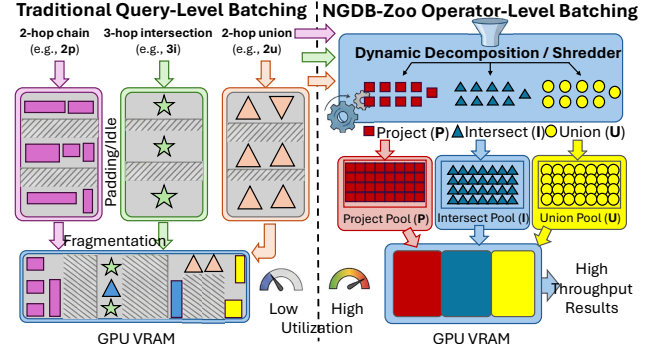


Figure 3. **Overcoming Topological Rigidity.** (Left): Query-level batching incurs high fragmentation overheads by segregating distinct query structures. (Right): NGDB-Zoo aggregates atomic operators into homogeneous Operator Pools for unified execution, eliminating structural constraints and saturating GPU cores.

Φ . For each entity $e_i \in \mathcal{E}$, its joint representation is $\mathbf{x}_i = [\mathbf{h}_i \oplus \Phi(d_i)] \in \mathcal{H}_{joint}$.

To integrate these features into probabilistic reasoning frameworks (e.g., BetaE), we interpret the joint signals as the sufficient statistics that parameterize entity distributions. We employ a trainable mapping network $\Psi_\theta : \mathcal{H}_{joint} \rightarrow \mathcal{D}$ to project the joint embeddings into the manifold \mathcal{D} :

$$[\alpha_i^0, \beta_i^0] = \Psi_\theta(\mathbf{x}_i) \quad (3)$$

where α_i^0, β_i^0 denote the initial Beta distribution parameters. These parameters then serve as the input for the subsequent sequence of logical operators (e.g., projection, intersection), ensuring that the entire reasoning chain is grounded in both learned topology and static semantic knowledge.

4. Method

To address the hardware efficiency bottlenecks and representational sparsity in Neural Graph Databases (NGDBs), we propose NGDB-Zoo. This framework decouples the logical query topology from hardware execution by decomposing complex queries into a unified pool of neural operators.

4.1. Operator-Level Batching

Standard query-level batching organizes computation by grouping queries with identical topological structures (e.g.,

grouping all 2-hop chains). However, this approach causes severe fragmentation when training on diverse query mixtures typical of Neural Agentic Databases and Neural Graph Databases. If the training distribution \mathcal{D} contains $|\mathcal{T}|$ distinct query structures, the effective batch size for any specific kernel is reduced by a factor of approximately $|\mathcal{T}|$. To resolve this bottleneck, we draw inspiration from Atom (Zhou et al., 2024), which introduced operator-level batching to optimize throughput in KG serving and inference systems. In Figure 3, we adapt this paradigm to the training phase of logical query embeddings. By shifting the abstraction level from the monolithic query to the atomic operator, we enable high-throughput training even the query workload is highly entropic and structurally diverse.

Graph Decomposition and Representation. We define a logical query q not as a monolithic sequence, but as a directed acyclic graph (DAG) $G_q = (V, E)$. Here, V represents the set of atomic operators (e.g., Project, Intersect, Union), and E represents the data dependencies between them. Formally, a complex query such as a 2-way intersection $q = \phi_{\cap}(\phi_p(e_1, r_1), \phi_p(e_2, r_2))$ is decomposed into independent projection nodes whose outputs flow into a central intersection node.

This decomposition allows us to aggregate operators v across disparate query structures into global execution pools \mathcal{P}_{τ} , where τ denotes the operator type (e.g., matrix-vector multiplication or set intersection).

Dynamic Scheduling. The core of our training engine is a dynamic scheduler that optimizes GPU occupancy. At any simulation step t , let \mathcal{R}_t be the set of all ready operators (those whose dependencies are satisfied). The scheduler groups \mathcal{R}_t by operator type τ and selects a target type τ^* to execute. We employ a *Max-Fitness* policy to maximize hardware utilization. We define the fitness ratio $\rho(\tau)$ as:

$$\rho(\tau) = \frac{|\{o \in \mathcal{R}_t : \text{type}(o) = \tau\}|}{B_{\max}} \quad (4)$$

where B_{\max} is the maximum efficient batch size for the hardware. The scheduler selects $\tau^* = \arg \max_{\tau} \rho(\tau)$, thereby prioritizing the operator type that most effectively saturates the GPU cores.

Batched Execution. Upon selecting the target type τ^* , the execution engine performs a *Cross-Query Operator Fusion*. Let $\{o_1, o_2, \dots, o_k\}$ be the set of operators in \mathcal{R}_t with $\text{type}(o_i) = \tau^*$. Regardless of their original query contexts, their input tensors $\mathbf{X} = \{\mathbf{x}_1, \mathbf{x}_2, \dots, \mathbf{x}_k\}$ are coalesced into a contiguous memory block to form a unified batch $\mathbf{X}_{\text{batch}} \in \mathbb{R}^{k \times d}$. This unified representation allows the engine to invoke a single high-performance GPU kernel:

$$\mathbf{Y}_{\text{batch}} = \text{Kernel}_{\tau^*}(\mathbf{X}_{\text{batch}}; \theta_{\tau^*}) \quad (5)$$

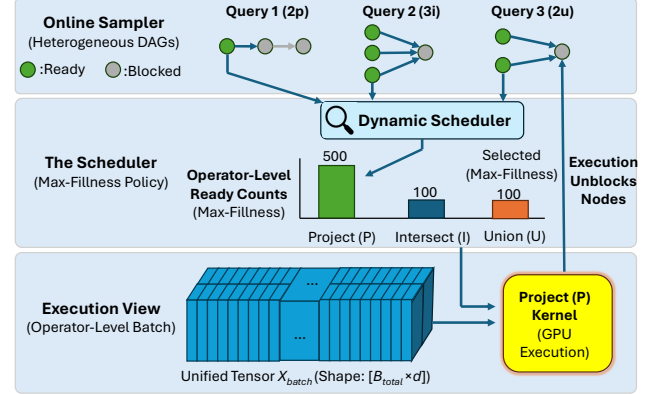


Figure 4. **Max-Fitness Dynamic Scheduling.** By prioritizing operator pools with the highest workload, the scheduler maximizes GPU utils. This dynamic selection effectively unblocks dependent nodes, ensuring a continuous, high-throughput training stream.

where θ_{τ^*} represents the shared parameters for the operator type. This mechanism effectively mitigates kernel launch overhead and eliminates branch divergence across heterogeneous query structures, ensuring that the hardware operates near its theoretical peak performance.

4.2. Vectorized Objective Optimization

Building on the QueryDAG abstraction, we implement a multi-phase optimization strategy that restructures the entire training lifecycle to maximize system throughput.

Vectorized Logit Formulation. Beyond structural scheduling, the computation of the objective function often suffers from high latency due to iterative embedding lookups. We reformulate the loss computation to leverage high-bandwidth memory (HBM). Instead of computing the scores for positive and negative samples individually, we represent the query embeddings and candidate entity embeddings as tensors $\mathbf{Q} \in \mathbb{R}^{B \times d}$ and $\mathbf{E} \in \mathbb{R}^{N \times d}$, respectively. The objective function calculation is then cast as a dense matrix-vector product:

$$\mathcal{L} = \sum_{i=1}^B \psi(\mathbf{Q}_i \cdot \mathbf{E}_{pos}^{\top}) + \sum_{i=1}^B \sum_{j \in \mathcal{N}_i} \psi(\mathbf{Q}_i \cdot \mathbf{E}_{neg,j}^{\top}) \quad (6)$$

where $\psi(\cdot)$ denotes the scoring function (e.g., Distance or Log-Sigmoid). This formulation allows the underlying linear algebra libraries to optimize data reuse via shared memory.

Efficient Tensor Indexing. To further alleviate CPU-GPU synchronization bottlenecks, we introduce a *Precomputed Indexing* mechanism. By pre-calculating the memory offsets for entity embeddings within the QueryDAG, we employ asynchronous scatter/gather operations. This replaces redundant tensor concatenation and splitting, ensuring that the

critical path of the forward and backward passes remains entirely within the accelerator’s memory space.

4.3. Efficient System Architecture and Optimization

To facilitate training on large-scale data with high-throughput requirements, we propose a multi-faceted system optimization framework. This framework addresses two primary bottlenecks: memory-intensive intermediate tensor management and sub-optimal hardware utilization during complex query reasoning.

Proactive Memory Management via Reference Counting.

To enable training with massive batch sizes, we implement Eager Reference Counting to achieve fine-grained resource reclamation. Formally, for any intermediate tensor T generated within a Query Directed Acyclic Graph (QueryDAG), let $\mathcal{V}_{\text{desc}}(T)$ denote the set of downstream operators that consume T as input, and let $\mathcal{F}_t \subseteq \mathcal{V}$ denote the set of operators that have been executed by scheduling step t . The system maintains a dynamic reference counter for each tensor. A tensor T is eligible for immediate memory deallocation at step t if and only if every consumer has already been executed:

$$\text{RECLAIM}(T) \iff \sum_{v \in \mathcal{V}_{\text{desc}}(T)} \mathbb{I}(v \notin \mathcal{F}_t) = 0 \quad (7)$$

By strictly enforcing this reclamation policy, our system significantly lowers the memory pressure compared to query-scoped allocation, enabling larger batch sizes training without triggering out-of-memory errors on modern hardware.

Asynchronous Parallelism and Pipelining. The memory efficiency gains from reference counting serve as a foundation for high-concurrency execution. We implement a decoupled execution pipeline characterized by two key parallelization strategies:

Multi-stream Operator Execution: We leverage independent CUDA streams to parallelize disjoint operator types within the QueryDAG. This allows for the simultaneous execution of compute-bound and memory-bound kernels, effectively masking hardware latency. *Heterogeneous Pipelining:* To handle massive graphs exceeding GPU capacity, we adopt an asynchronous CPU-GPU pipelining strategy inspired by SMORE (Ren et al., 2022). Feature and structure embeddings are stored in host memory (CPU) and asynchronously fetched to pinned memory before scatter-gathering to the GPU. To mitigate the bottleneck of CPU-side data preparation, we use a consumer-producer pipeline. While the GPU executes current operator batches, the CPU concurrently performs asynchronous sampling for subsequent queries, ensuring a continuous data flow to the accelerators.

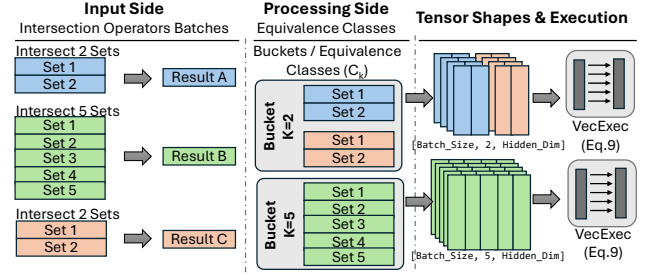


Figure 5. **Vectorized execution for Intersection/Union.** By grouping operations into cardinality-based Equivalence Classes, we eliminate tensor misalignment. This enables perfectly aligned **Vectorized Execution**, replacing slow loops with dense matrix operations.

Efficiency-oriented Intersect and Union Operator.

As shown in Figure 5, unlike structural operators with fixed input degrees (e.g., *Projection* or *Negation*), the *Intersection* (\cap) and *Union* (\cup) operators in logical reasoning encounter variable-cardinality inputs, which typically leads to fragmented memory allocation and sub-optimal GPU utilization. To handle the computational complexity of the Intersect and Union Operator, we propose a batching strategy based on input cardinality. Let $\Phi \in \{\mathcal{O}_{\text{int}}, \mathcal{O}_{\text{un}}\}$ denote a set-based operator acting on an arbitrary number of input embeddings $\mathcal{S} = \{\mathbf{e}_1, \dots, \mathbf{e}_n\}$. We define the computation over a query batch as a partition into equivalence classes $\{\mathcal{C}_k\}_{k \in \mathcal{K}}$, where each class \mathcal{C}_k clusters operations with identical input cardinality $k = |\mathcal{S}|$:

$$\mathcal{C}_k = \{\phi_i \in \text{Batch} \mid \text{card}(\text{input}(\phi_i)) = k\}. \quad (8)$$

The global operation is then reformulated as a sequence of vectorized executions:

$$\mathcal{O}_\Phi = \bigoplus_{k \in \mathcal{K}} \text{VecExec}(\mathcal{C}_k), \quad (9)$$

where $\text{VecExec}(\cdot)$ denotes a synchronized tensor operation on a k -depth stacked tensor. This grouping mechanism optimizes GPU memory utilization and maximizes throughput by reducing fragmented memory allocations.

Online Data Sampling and Test Time Optimization.

For NGDBs on large-scale graphs, the query space is effectively infinite, making the storage of pre-computed datasets prohibitive. Consequently, we employ an online data sampling system that generates queries dynamically during training. Beyond eliminating storage overhead, this approach exploits temporal locality in query streams. By adjusting the sampling distribution on-the-fly based on query difficulty, the system can optimize for specific query patterns that appear in bursts during multi-run training sessions. This dynamic generation allows for an unlimited stream of diverse samples and enables the curriculum to adaptively prioritize complex multi-hop structures to stabilize convergence.

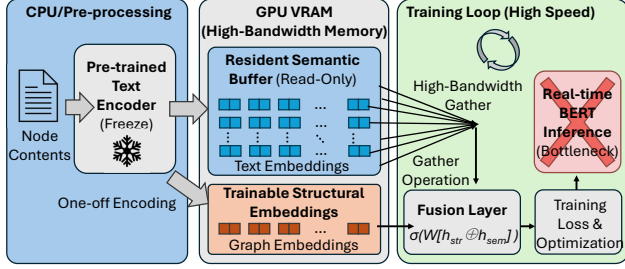


Figure 6. **Illustration of the decoupled semantic integration strategy.** By relegating the heavy text encoder (PTE) to an offline pre-computation phase and caching embeddings in GPU memory, NGDB-Zoo achieves minimal-overhead semantic fusion during training.

4.4. Efficient Integration of Semantic Entity Representations

To augment entities with rich textual knowledge, we integrate high-dimensional semantic priors derived from Pre-trained Text Encoders (PTEs). However, joint training with PTEs typically incurs prohibitive overheads, transforming high-throughput graph reasoning into a compute-bound or I/O-bound bottleneck. To resolve this, we propose a *decoupled, GPU-resident integration strategy* that ensures the training loop remains strictly inference-free.

Decoupled Semantic Encoding. Instead of performing real-time feature extraction, which couples the heavy PTE inference with the gradient descent loop, we relegate semantic acquisition to an *offline pre-computation phase*. Given an entity set \mathcal{E} , we employ a frozen PTE $\Phi(\cdot)$ to map each entity $e_i \in \mathcal{E}$ to a high-dimensional latent space:

$$\mathcal{H}^{sem} = \{\Phi(T_i) \mid e_i \in \mathcal{E}\} \in \mathbb{R}^{|\mathcal{E}| \times d_i} \quad (10)$$

where T_i denotes the textual description of entity e_i . Crucially, once \mathcal{H}^{sem} is generated, the PTE $\Phi(\cdot)$ is **unloaded** from memory. This decoupling ensures that the subsequent training phase is completely agnostic to the complexity of the text encoder.

High-Throughput GPU-Resident Integration. To eliminate the latency of CPU-to-GPU data transfer (PCIe bandwidth bottleneck), we implement a *GPU-resident caching mechanism*. The global semantic manifold \mathcal{H}^{sem} is registered as a persistent, non-trainable buffer directly within the GPU’s High Bandwidth Memory (HBM).

Consequently, for a mini-batch of entity indices \mathcal{I} , the integration of semantic features is reduced from a model inference task to a high-speed tensor indexing operation:

$$\mathbf{E}_{batch}^{sem} = \text{Gather}(\mathcal{H}^{sem}, \mathcal{I}) \quad (11)$$

This design achieves *minimal-overhead* data access. To align these high-dimensional priors with the structural embedding space, we employ a lightweight linear projection

$$\mathcal{F} : \mathbb{R}^{d_i} \rightarrow \mathbb{R}^d:$$

$$\mathbf{e}_i^{fused} = \sigma(\mathbf{W}_p[\mathbf{h}_i^{str} \oplus \mathcal{F}(\mathbf{h}_i^{sem})] + \mathbf{b}_p) \quad (12)$$

where \oplus denotes concatenation and \mathbf{h}_i^{str} is the learnable structural embedding. By treating semantic integration as a pure memory lookup, our framework sustains peak GPU utilization regardless of the PTE’s original size.

5. Experiments

5.1. Experimental Setup

Baselines training framework. We compare our single-hop KG completion runtime with state-of-the-art frameworks SQE (Bai et al., 2023), SMORE (Ren et al., 2022), DGL-KE (Zheng et al., 2020), Pytorch-Bigraph (PBG) (Lerer et al., 2019), and Marius (Mohoney et al., 2021). Then we evaluate the end-to-end training performance of NGDB-Zoo on multi-hop reasoning over both small and large KGs.

Backbone models. To validate the effectiveness of our training framework across diverse representational paradigms, we benchmark against a comprehensive suite of query encoding models. These baselines parameterize logical operators using various geometric and neural structures: **GQE** (Hamilton et al., 2018) and **Q2P** (Bai et al., 2022) utilize vector-based representations; **Q2B** (Ren et al., 2020) and **BetaE** (Ren & Leskovec, 2020) leverage Beta distributions for probabilistic reasoning; and **FuzzQE** (Chen et al., 2022b) applies fuzzy logic principles. For pretrained text encoder, we use Qwen3-Embedding-0.6B (Zhang et al., 2025) and BGE-Base-En-v1.5 (Xiao et al., 2023).

Dataset. Experiments were conducted on following benchmarks: FB15k, FB15k-237, NELL (Ren & Leskovec, 2020), FB400k (Talmor & Berant, 2018), ogbl-wikikg2 (Hu et al., 2020a), and Atlas-Wiki (Bai et al., 2025a). We used the validation and test queries for the first three datasets. For ogbl-wikikg2, queries were randomly sampled using official edge splits. For FB400k, we utilized SPARQL annotations from CWQ as queries, following the data splitting method in SMORE (Ren et al., 2022). For ATLAS-Wiki-Triple-4M, queries were sampled using degree-weighted edge sampling. Dataset statistics are listed in Table 4 in Appendix C.

Framework and Hardware. Our framework is implemented using PyTorch 2.0 and Python 3.10. Code will be released upon publication. Unless otherwise stated, all other experiments are conducted on NVIDIA A6000 GPUs (48GB memory) with 40 CPU cores.

Table 1. Scalability and Predictive Performance on Massive Knowledge Graphs. We report the filtered MRR (%), training throughput (10^3 Queries/sec), and peak GPU memory occupancy (GB) across three production-scale datasets. NGDB-Zoo enables high throughput and robust reasoning across diverse paradigms on production-scale graphs with millions of entities.

Dataset	Model	MRR (%)	TPut (\uparrow)	Mem (GB \downarrow)
FB400k	GQE	35.84	24.68	7.5
	Q2B	52.33	21.55	11.0
	BetaE	50.40	19.97	14.0
ogbl-wikikg2	GQE	32.88	23.92	8.0
	Q2B	42.01	20.75	11.0
	BetaE	44.54	19.65	14.0
ATLAS-Wiki-Triple-4M	GQE	7.31	22.00	10.0
	Q2B	9.22	18.47	12.0
	BetaE	9.01	17.89	15.0

5.2. Scalability

GPU memory and end-to-end training speed. We test NGDB-Zoo on all six KGs and report the end-to-end training speed and GPU memory data. As reported in Table 3, NGDB-Zoo achieves substantial throughput gains compared to representative baselines. For instance, on the FB15k dataset using the BetaE model, our system attains 4,477 queries/sec, representing a $7.0\times$ speedup over the SQE framework. While NGDB-Zoo exhibits higher GPU memory footprints compared to SMORE due to our GPU-resident caching strategy, the memory usage remains well within the capacity of modern accelerators and often stays significantly lower than SQE in complex scenarios like NELL995. As shown in Table 1, this efficiency extends to massive KGs, where NGDB-Zoo sustains high throughput even with million-level entities, proving its viability for production-scale neural graph databases.

Multi-GPU speed up. We report the training speed-up on 1, 2, 4, and 8 GPUs across different methods on the ogbl-wikikg2 and ATLAS-Wiki-Triple-4M in Figure 7. The training throughput increases almost linearly with the number of GPUs, demonstrating that our toolkit is highly scalable and the communication overhead is minimal.

Single-hop link prediction completion runtime. Here we compare the single-hop link prediction (KG completion) runtime performance with state-of-the-art large-scale KG frameworks including Marius, PBG and SMORE. We report the results for ComplEx model with 100 embedding dimension on Freebase. We use the same multi-GPU V100 configuration as in Marius, and the current official release versions are also the same. For baseline results, we reuse Table 5 from Ren et al. (2022). As shown in Table 2, NGDB-Zoo achieves significantly faster runtime in 1-GPU setting than PBG. Also it scales better than the other systems, while

Table 2. Runtime performance on Freebase KG. *Results taken from Mohoney et al. (2021) and Ren et al. (2022) with the same V100 GPUs.

System	Epoch Time (s)			
	1-GPU	2-GPU	4-GPU	8-GPU
Marius (Mohoney et al., 2021)*	727	-	-	-
PBG (Lerer et al., 2019)*	3060	1400	515	419
SMORE (Ren et al., 2022)*	760	411	224	121
NGDB-Zoo (Ours)	628	322	181	94

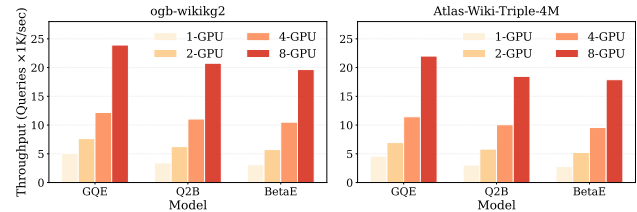


Figure 7. Multi-GPU Throughput Scalability. Training throughput increases near-linearly with the number of GPUs across ogbl-wikikg2 and ATLAS-Wiki-Triple-4M. Units are in # Queries (x1K/sec).

Marius does not officially support multi-GPU parallel training functionality at the current stage.

5.3. Predictive performance

Calibration on small KGs. We first evaluate our NGDB-Zoo system for five representational paradigms (BetaE, Q2B, GQE, Q2P, and FuzzQE) on the three small benchmark datasets created in BetaE. For a fair comparison, we test our system against other frameworks under identical online sampler. To determine the system’s throughput, we record both the data loading and sampling durations during this process. As summarized in Table 3, NGDB-Zoo consistently outperforms or matches competitive baselines in terms of MRR, demonstrating that training on dynamic online streams does not compromise reasoning accuracy.

Query answering on large KGs. We further evaluate NGDB-Zoo on three large-scale benchmarks: FB400k, ogbl-wikikg2, and ATLAS-Wiki-4M. As summarized in Table 1, NGDB-Zoo successfully scales diverse representational paradigms to graphs with millions of entities. On ogbl-wikikg2, BetaE attains the highest performance with an MRR of 44.54%, while Q2B demonstrates superior expressivity on FB400k, achieving 52.33%. This shows our system maintains robust reasoning even on the massive graph which contains over 4 million entities.

Online Sampling. To validate our adaptive approach, we conducted controlled experiments using a steered query distribution characterized by an abrupt spike in query difficulty every 15,000 training steps. As shown in Figure 9, our adaptive sampling mechanism consistently outperforms the baseline across all configurations. It achieves an average relative improvement of 21.5% in MRR. This indicates that adap-

Table 3. Performance comparison of NGDB-Zoo vs. KGReasoning, SMORE and SQE.

Dataset	Model	MRR (%)				Training queries (Queries/Sec)				GPU Memory (GB)			
		KGR	SMORE	SQE	NGDB-Zoo	KGR	SMORE	SQE	NGDB-Zoo	KGR	SMORE	SQE	NGDB-Zoo
FB15k	BetaE	41.60	40.39	40.82	43.04	291	2808	636	4477	2.68	1.16	8.05	12.95
	Q2B	38.00	41.54	41.08	42.85	855	3588	343	4086	1.32	0.96	6.01	5.07
	GQE	28.00	30.60	29.21	30.39	1395	3770	4598	6271	0.76	1.09	8.03	11.33
	Q2P	-	-	44.30	46.90	-	-	832	1940	-	-	4.76	11.41
	FuzzQE	-	-	42.17	42.33	-	-	720	2973	-	-	20.14	8.45
FB15k-237	BetaE	20.90	19.67	20.92	21.11	178	1633	655	4750	2.68	1.14	6.03	9.81
	Q2B	20.10	20.42	19.05	20.19	428	3115	343	4663	1.3	0.93	6.04	5.09
	GQE	16.30	15.68	16.75	16.98	1433	2882	1910	6034	0.75	1.02	8.01	9.77
	Q2P	-	-	20.12	22.08	-	-	842	1884	-	-	4.22	11.34
	FuzzQE	-	-	21.07	21.35	-	-	1350	2934	-	-	17.02	8.54
NELL995	BetaE	24.60	23.17	23.43	24.90	166	1807	154	4640	3.42	1.28	35.02	6.81
	Q2B	22.90	21.84	22.21	23.79	765	1926	82	4521	1.5	1	25.04	5.14
	GQE	18.60	17.53	18.02	18.89	1224	3691	2959	6329	1.01	1.17	45.04	7.12
	Q2P	-	-	23.18	25.65	-	-	836	2309	-	-	9.69	9.56
	FuzzQE	-	-	24.31	25.88	-	-	2165	2680	-	-	8.07	8.16
Average Without Q2P/FuzzQE		25.67	25.65	25.72	26.90	748	2802	1298	5086	1.71	1.08	16.36	8.12

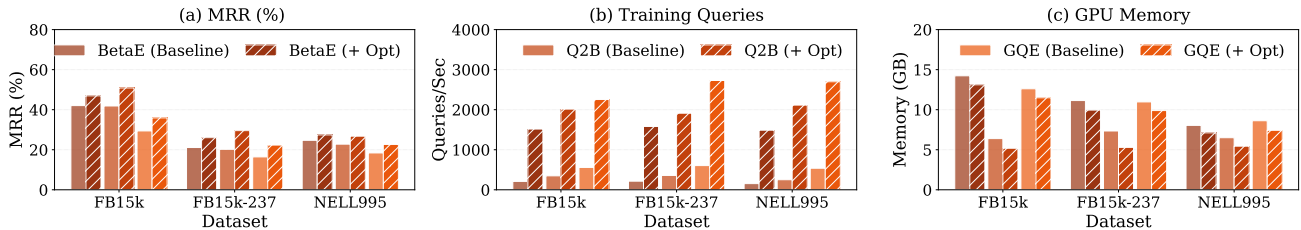


Figure 8. **Impact of Decoupled Semantic Integration.** We compare the standard joint training (Solid) against our GPU-Resident Decoupled strategy (Hatched //) across three datasets and models. **(a) Predictive Performance:** Our method consistently improves MRR than without semantic priors by leveraging semantic priors. **(b) Throughput:** By removing the heavy Text Encoder from the training loop, we achieve a **5x-7x speedup**. **(c) Memory:** Despite caching embeddings, peak memory is reduced because the encoder is unloaded. Note: Higher is better for (a)&(b); lower is better for (c).

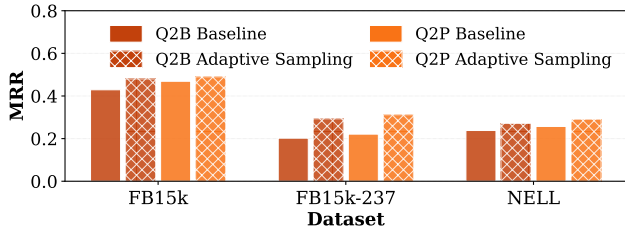


Figure 9. Performance comparison with and without Adaptive Sampling. Adaptive Sampling consistently improves MRR over all models and datasets.

tive sampling demonstrates superior robustness in handling non-stationary distributions by rapidly accommodating sudden difficulty shifts. This dynamic generation facilitates an unlimited stream of diverse samples, enabling the model to adaptively prioritize complex multi-hop structures and stabilize convergence in highly entropic environments.

5.4. Impact of Decoupled Semantic Augmentation

Throughput, Memory and Predictive Performance. On standard benchmarks (FB15k, NELL) where the full manifold fits in VRAM, we utilize the GPU-Resident strategy to maximize throughput by eliminating PCIe latency. We evaluate the impact of our decoupled semantic integration

strategy across three models: BetaE, Q2B, and GQE. Figure 8 illustrates the substantial performance boost observed with the Qwen3-Embedding. Furthermore, as detailed in Appendix Table 8, these trends remain consistent when utilizing BGE-Base-En-v1.5. Across both encoders, the optimizations consistently yield a 5x-7x throughput speedup and reduce memory consumption. **Throughput:** By shifting the computationally expensive text encoder inference to an offline phase and caching embeddings in GPU memory, we achieve a **5x-7x speedup** in training throughput. This confirms that our “inference-free” design effectively eliminates the computational bottleneck. **Memory:** Despite caching the full entity manifold on-device, the overall GPU memory footprint decreases. This is because the massive Pre-trained Text Encoder (PTE) is completely **unloaded** from VRAM during training, offsetting the storage cost of the embedding buffer. **Predictive Performance:** Semantic Entity Joint Training consistently improve MRR across all models and datasets by harnessing linguistic priors.

6. Conclusion

We presented NGDB-Zoo, a framework resolving the efficiency-expressivity tension in Neural Graph Databases. By adopting operator-level batching, NGDB-Zoo over-

comes topological rigidity, achieving leading throughput and near-linear multi-GPU scalability. We also showed that integrating Pre-trained Text Encoders alleviates representation friction in sparse graphs. Despite a modest memory increase, NGDB-Zoo sustains robust reasoning on massive graphs, offering a scalable foundation for next-generation neuro-symbolic systems.

Impact Statement

This paper presents work whose goal is to advance the field of Machine Learning. There are many potential societal consequences of our work, none which we feel must be specifically highlighted here.

References

- Bai, J., Wang, Z., Zhang, H., and Song, Y. Query2particles: Knowledge graph reasoning with particle embeddings. *arXiv preprint arXiv:2204.12847*, 2022.
- Bai, J., Zheng, T., and Song, Y. Sequential query encoding for complex query answering on knowledge graphs. *arXiv preprint arXiv:2302.13114*, 2023.
- Bai, J., Fan, W., Hu, Q., Zong, Q., Li, C., Tsang, H. T., Luo, H., Yim, Y., Huang, H., Zhou, X., et al. Autoschemakg: Autonomous knowledge graph construction through dynamic schema induction from web-scale corpora. *arXiv preprint arXiv:2505.23628*, 2025a.
- Bai, J., Wang, Z., Zhou, Y., Yin, H., Fei, W., Hu, Q., Deng, Z., Cheng, J., Zheng, T., Tsang, H. T., et al. Top ten challenges towards agentic neural graph databases. *arXiv preprint arXiv:2501.14224*, 2025b.
- Bao, T., Ye, X., Ruan, H., Liu, C., Wu, W., and Yan, J. Beyond circuit connections: A non-message passing graph transformer approach for quantum error mitigation. In *The Thirteenth International Conference on Learning Representations*, 2025.
- Besta, M., Iff, P., Scheidl, F., Osawa, K., Dryden, N., Podstawski, M., Chen, T., and Hoefler, T. Neural graph databases. In *Learning on Graphs Conference*, pp. 31–1. PMLR, 2022.
- Chen, D., O’Bray, L., and Borgwardt, K. Structure-aware transformer for graph representation learning. In *International conference on machine learning*, pp. 3469–3489. PMLR, 2022a.
- Chen, D., Krimmel, M., and Borgwardt, K. Flatten graphs as sequences: Transformers are scalable graph generators. *arXiv preprint arXiv:2502.02216*, 2025a.
- Chen, H., Wang, X., Zhang, Z., Li, H., Feng, L., and Zhu, W. Autogfm: Automated graph foundation model with adaptive architecture customization. In *Forty-second International Conference on Machine Learning*, 2025b.
- Chen, S., Wei, S., Liu, C., and Yang, W. Dycl: Dynamic neural network compilation via program rewriting and graph optimization. In *Proceedings of the 32nd ACM SIGSOFT International Symposium on Software Testing and Analysis*, pp. 614–626, 2023.
- Chen, X., Hu, Z., and Sun, Y. Fuzzy logic based logical query answering on knowledge graphs. In *Proceedings of the AAAI Conference on Artificial Intelligence*, volume 36, pp. 3939–3948, 2022b.
- Choi, D., Kim, S., Kim, J., Kim, K., Lee, G., Kang, S., Kim, M., and Shin, K. Rdb2g-bench: A comprehensive benchmark for automatic graph modeling of relational databases. *arXiv preprint arXiv:2506.01360*, 2025.
- Choudhary, N., Rao, N., Katariya, S., Subbian, K., and Reddy, C. K. Self-supervised hyperboloid representations from logical queries over knowledge graphs. In *Proceedings of the web conference 2021*, pp. 1373–1384, 2021.
- Cui, X., Peng, C. W., Kuek, A., and Lim, S.-N. Improving soft unification with knowledge graph embedding methods. In *Forty-second International Conference on Machine Learning*, 2025.
- Feng, T., Wu, Y., Lin, G., and You, J. Graph world model. *arXiv preprint arXiv:2507.10539*, 2025.
- Finder, S. E., Weber, R. S., Eliasof, M., Freifeld, O., and Treister, E. Improving the effective receptive field of message-passing neural networks. *arXiv preprint arXiv:2505.23185*, 2025.
- Galkin, M., Trivedi, P., Maheshwari, G., Usbeck, R., and Lehmann, J. Message passing for hyper-relational knowledge graphs. *arXiv preprint arXiv:2009.10847*, 2020.
- Galkin, M., Yuan, X., Mostafa, H., Tang, J., and Zhu, Z. Towards foundation models for knowledge graph reasoning. *arXiv preprint arXiv:2310.04562*, 2023.
- Galkin, M., Zhou, J., Ribeiro, B., Tang, J., and Zhu, Z. A foundation model for zero-shot logical query reasoning. *Advances in Neural Information Processing Systems*, 37: 54137–54160, 2024.
- Ge, X., Wang, Y. C., Wang, B., Kuo, C.-C. J., et al. Knowledge graph embedding: An overview. *APSIPA Transactions on Signal and Information Processing*, 13(1), 2024.
- Hamilton, W., Bajaj, P., Zitnik, M., Jurafsky, D., and Leskovec, J. Embedding logical queries on knowledge graphs. *Advances in neural information processing systems*, 31, 2018.
- He, L., Li, C., Tang, P., and Su, S. Going deeper into locally differentially private graph neural networks. In *Forty-second International Conference on Machine Learning*, 2025.
- Hu, Q., Jiang, W., Li, H., Wang, Z., Bai, J., Mao, Q., Song, Y., Fan, L., and Li, J. Federated neural graph databases. *arXiv preprint arXiv:2402.14609*, 2024a.

- Hu, Q., Li, H., Bai, J., Wang, Z., and Song, Y. Privacy-preserved neural graph databases. In *Proceedings of the 30th ACM SIGKDD Conference on Knowledge Discovery and Data Mining*, pp. 1108–1118, 2024b.
- Hu, W., Fey, M., Zitnik, M., Dong, Y., Ren, H., Liu, B., Catasta, M., and Leskovec, J. Open graph benchmark: Datasets for machine learning on graphs. *Advances in neural information processing systems*, 33:22118–22133, 2020a.
- Hu, Z., Dong, Y., Wang, K., and Sun, Y. Heterogeneous graph transformer. In *Proceedings of the web conference 2020*, pp. 2704–2710, 2020b.
- Ketata, M. A., Lüdke, D., Schwinn, L., and Günnemann, S. Joint relational database generation via graph-conditional diffusion models. *arXiv preprint arXiv:2505.16527*, 2025.
- Kim, J., Nguyen, D., Min, S., Cho, S., Lee, M., Lee, H., and Hong, S. Pure transformers are powerful graph learners. *Advances in Neural Information Processing Systems*, 35: 14582–14595, 2022.
- Kim, J. H., Kim, S., Moon, S., Kim, H., Woo, J., and Kim, W. Y. Discrete diffusion schrödinger bridge matching for graph transformation. *arXiv preprint arXiv:2410.01500*, 2024.
- Lefebvre, F. and Varoquaux, G. Scalable feature learning on huge knowledge graphs for downstream machine learning. *arXiv preprint arXiv:2507.00965*, 2025.
- Lerer, A., Wu, L., Shen, J., Lacroix, T., Wehrstedt, L., Bose, A., and Peysakhovich, A. Pytorch-biggraph: A large-scale graph embedding system. 2019.
- Li, Y., Guo, Z., Li, G., and Li, B. You only spectralize once: Taking a spectral detour to accelerate graph neural network. In *The Thirty-ninth Annual Conference on Neural Information Processing Systems*, 2025.
- Min, E., Chen, R., Bian, Y., Xu, T., Zhao, K., Huang, W., Zhao, P., Huang, J., Ananiadou, S., and Rong, Y. Transformer for graphs: An overview from architecture perspective. *arXiv preprint arXiv:2202.08455*, 2022.
- Mohoney, J., Waleffe, R., Xu, H., Rekatsinas, T., and Venkataraman, S. Marius: Learning massive graph embeddings on a single machine. In *15th USENIX Symposium on Operating Systems Design and Implementation (OSDI 21)*, 2021.
- Ott, M., Edunov, S., Baevski, A., Fan, A., Gross, S., Ng, N., Grangier, D., and Auli, M. fairseq: A fast, extensible toolkit for sequence modeling. *arXiv preprint arXiv:1904.01038*, 2019.
- Pengmei, Z., Shen, Z., Wang, Z., Collins, M., and Rangwala, H. Pushing the limits of all-atom geometric graph neural networks: Pre-training, scaling and zero-shot transfer. *arXiv preprint arXiv:2410.21683*, 2024.
- Ramezanpour, R., Tenorio, V. M., Marques, A. G., Sabharwal, A., and Segarra, S. A few moments please: Scalable graphon learning via moment matching. *arXiv preprint arXiv:2506.04206*, 2025.
- Ren, H. and Leskovec, J. Beta embeddings for multi-hop logical reasoning in knowledge graphs. *Advances in Neural Information Processing Systems*, 33:19716–19726, 2020.
- Ren, H., Hu, W., and Leskovec, J. Query2box: Reasoning over knowledge graphs in vector space using box embeddings. *arXiv preprint arXiv:2002.05969*, 2020.
- Ren, H., Dai, H., Dai, B., Chen, X., Zhou, D., Leskovec, J., and Schuurmans, D. Smore: Knowledge graph completion and multi-hop reasoning in massive knowledge graphs. In *Proceedings of the 28th ACM SIGKDD conference on knowledge discovery and data mining*, pp. 1472–1482, 2022.
- Ren, H., Galkin, M., Cochez, M., Zhu, Z., and Leskovec, J. Neural graph reasoning: Complex logical query answering meets graph databases. *arXiv preprint arXiv:2303.14617*, 2023.
- Rong, Y., Bian, Y., Xu, T., Xie, W., Wei, Y., Huang, W., and Huang, J. Self-supervised graph transformer on large-scale molecular data. *Advances in neural information processing systems*, 33:12559–12571, 2020.
- Shi, Z., Wang, J., Zhuang, Z., Liang, X., Li, B., and Wu, F. Accurate and scalable graph neural networks via message invariance. *arXiv preprint arXiv:2502.19693*, 2025.
- Sun, Z., Deng, Z.-H., Nie, J.-Y., and Tang, J. Rotate: Knowledge graph embedding by relational rotation in complex space. *arXiv preprint arXiv:1902.10197*, 2019.
- Talmor, A. and Berant, J. The web as a knowledge-base for answering complex questions. *arXiv preprint arXiv:1803.06643*, 2018.
- Tang, B., Liu, Z., Jiang, K., Chen, S., and Dong, X. Training-free message passing for learning on hypergraphs. *arXiv preprint arXiv:2402.05569*, 2024.
- Trouillon, T., Welbl, J., Riedel, S., Gaussier, É., and Bouchard, G. Complex embeddings for simple link prediction. In *International conference on machine learning*, pp. 2071–2080. PMLR, 2016.
- Veen, A. H. Dataflow machine architecture. *ACM Computing Surveys (CSUR)*, 18(4):365–396, 1986.

- Wang, K., Reimers, N., and Gurevych, I. Tsdad: Using transformer-based sequential denoising auto-encoder for unsupervised sentence embedding learning. *arXiv preprint arXiv:2104.06979*, 2021a.
- Wang, L., Zhao, W., Wei, Z., and Liu, J. Simkgc: Simple contrastive knowledge graph completion with pre-trained language models. *arXiv preprint arXiv:2203.02167*, 2022.
- Wang, X., Gao, T., Zhu, Z., Zhang, Z., Liu, Z., Li, J., and Tang, J. Kepler: A unified model for knowledge embedding and pre-trained language representation. *Transactions of the Association for Computational Linguistics*, 9: 176–194, 2021b.
- Wang, Y., Wang, X., Gan, Q., Wang, M., Yang, Q., Wipf, D., and Zhang, M. Griffin: Towards a graph-centric relational database foundation model. *arXiv preprint arXiv:2505.05568*, 2025.
- Wei, Q., Morrell, E., Goetz, L., and van der Schaar, M. Semantic-kg: Using knowledge graphs to construct benchmarks for measuring semantic similarity. *arXiv preprint arXiv:2511.19925*, 2025.
- Wu, Y., Xu, Y., Zhang, W., Xu, X., and Zhang, Y. Query2gmm: Learning representation with gaussian mixture model for reasoning over knowledge graphs. In *Proceedings of the ACM web conference 2024*, pp. 2149–2158, 2024.
- Wu, Z., Pan, S., Chen, F., Long, G., Zhang, C., and Yu, P. S. A comprehensive survey on graph neural networks. *IEEE transactions on neural networks and learning systems*, 32 (1):4–24, 2020.
- Xiao, S., Liu, Z., Zhang, P., and Muennighoff, N. C-pack: Packaged resources to advance general chinese embedding, 2023.
- Xiong, B., Nayyeri, M., Jin, M., He, Y., Cochez, M., Pan, S., and Staab, S. Geometric relational embeddings: A survey. *arXiv preprint arXiv:2304.11949*, 2023.
- Yan, Y., Hu, F., Chen, J., Bhendawade, N., Ye, T., Gong, Y., Duan, N., Cui, D., Chi, B., and Zhang, R. Fast-seq: Make sequence generation faster. *arXiv preprint arXiv:2106.04718*, 2021.
- Yang, B., Yih, W.-t., He, X., Gao, J., and Deng, L. Embedding entities and relations for learning and inference in knowledge bases. *arXiv preprint arXiv:1412.6575*, 2014.
- Yang, D., Qing, P., Li, Y., Lu, H., and Lin, X. Gammae: Gamma embeddings for logical queries on knowledge graphs. *arXiv preprint arXiv:2210.15578*, 2022.
- Yao, L., Mao, C., and Luo, Y. Kg-bert: Bert for knowledge graph completion. *arXiv preprint arXiv:1909.03193*, 2019.
- Yun, S., Jeong, M., Kim, R., Kang, J., and Kim, H. J. Graph transformer networks. *Advances in neural information processing systems*, 32, 2019.
- Zeng, B., Wang, Q., Yan, M., Liu, Y., Chengze, R., Zhang, Y., Liu, H., Wang, Z., and Sun, H. Phympgn: Physics-encoded message passing graph network for spatiotemporal pde systems. *arXiv preprint arXiv:2410.01337*, 2024.
- Zhang, Y., Li, M., Long, D., Zhang, X., Lin, H., Yang, B., Xie, P., Yang, A., Liu, D., Lin, J., Huang, F., and Zhou, J. Qwen3 embedding: Advancing text embedding and reranking through foundation models. *arXiv preprint arXiv:2506.05176*, 2025.
- Zhang, Z., Wang, J., Chen, J., Ji, S., and Wu, F. Cone: Cone embeddings for multi-hop reasoning over knowledge graphs. *Advances in Neural Information Processing Systems*, 34:19172–19183, 2021.
- Zheng, D., Song, X., Ma, C., Tan, Z., Ye, Z., Dong, J., Xiong, H., Zhang, Z., and Karypis, G. Dgl-ke: Training knowledge graph embeddings at scale. In *Proceedings of the 43rd International ACM SIGIR Conference on Research and Development in Information Retrieval*, pp. 739–748, 2020.
- Zheng, X., Huang, W., Zhou, C., Li, M., and Pan, S. Test-time graph neural dataset search with generative projection. In *Forty-second International Conference on Machine Learning*, 2025.
- Zhou, Q., Yin, P., Yan, X., Li, C., Jiang, G., and Cheng, J. Atom: An efficient query serving system for embedding-based knowledge graph reasoning with operator-level batching. *Proceedings of the ACM on Management of Data*, 2(4):1–29, 2024.

A. Limitations and Future Work

Despite its efficiency, the current architecture relies on a frozen text encoder. Future research could explore lightweight end-to-end co-optimization of the semantic and structural subspaces. System Trade-offs. To scale to massive graphs with limited VRAM, our current implementation on 4M-node graphs relies on asynchronous CPU-offloading. While effective, this introduces a dependency on PCIe bandwidth, which may become a bottleneck for even larger graphs or larger batch sizes compared to a fully GPU-resident approach. Furthermore, the reliance on a frozen text encoder decouples semantic understanding from structural learning, potentially limiting the model’s ability to adapt linguistic priors to specific graph topologies. Additionally, extending the operator-level paradigm to streaming knowledge bases, where the topology evolves in real-time, remains a promising direction for achieving truly autonomous graph reasoning.

A.1. Pretrained Embeddings for Structured Knowledge

Language Models for KGs. Recent work has explored combining pretrained language models with knowledge graphs: KG-BERT (Yao et al., 2019) uses BERT for triple classification. KEPLER (Wang et al., 2021b) jointly trains language models with KG embeddings. SimKGC (Wang et al., 2022) uses contrastive learning to align entity descriptions with KG structure. UltraQuery (Galkin et al., 2024) build pre-trained GNN foundation model for inductive reasoning on KGs.

Semantic Embeddings. Pretrained sentence transformers (Wang et al., 2021a) provide high-quality semantic embeddings. Recent models like Qwen3-Embedding (Zhang et al., 2025) achieve state-of-the-art performance on semantic similarity tasks. However, integrating these semantic representations with complex multi-hop reasoning models remains an open challenge.

B. Algorithm

In Algorithm 1, we presented our NGDB-Zoo in the form of pseudo-code to illustrate how it works.

Algorithm 1 Operator-Level Dynamic Scheduling Training Loop

Require: Batch of Queries \mathcal{Q} , Model Parameters Θ , Max Batch Size B_{\max}

```

1:  $\mathcal{G} \leftarrow \bigcup_{q \in \mathcal{Q}} \text{BUILDDAG}(q)$  {Construct fused computation graph}
2:  $\mathcal{G} \leftarrow \mathcal{G} \cup \text{ADDGRADIENTNODES}(\mathcal{G})$  {Include backward operators}
3: Initialize operator pools  $\mathcal{P}_\tau$  for each operator type  $\tau$ 
4: Initialize ready set  $\mathcal{R} \leftarrow \{v \in \mathcal{G} \mid \text{indegree}(v) = 0\}$ 
5: while  $\mathcal{R}$  is not empty do
6:   Distribute  $v \in \mathcal{R}$  into pools  $\mathcal{P}_{\text{TYPE}(v)}$ 
7:    $\mathcal{R} \leftarrow \emptyset$  {Clear ready set, wait for next cycle}
8:   Select  $\tau^* \leftarrow \arg \max_\tau \rho(\tau)$  {Apply Max-Fitness Policy}
9:    $\mathcal{B} \leftarrow \text{POPBATCH}(\mathcal{P}_{\tau^*}, B_{\max})$ 
10:   $\mathbf{O} \leftarrow \text{EXECUTEKERNEL}(\mathcal{B}, \Theta)$  {Fused GPU Kernel}
11:  for  $o_i \in \mathcal{B}$  do
12:     $o_i.\text{output} \leftarrow \mathbf{O}_i$ 
13:     $\text{DECREMENTREFCOUNTS}(\text{INPUTS}(o_i))$  {Eager Reclamation}
14:    for  $v_{\text{succ}} \in \text{SUCCESSORS}(o_i)$  do
15:      if  $\text{DEPENDENCIESMET}(v_{\text{succ}})$  then
16:         $\mathcal{R} \leftarrow \mathcal{R} \cup \{v_{\text{succ}}\}$  {Update ready set}
17:      end if
18:    end for
19:  end for
20: end while
21:  $\text{OPTIMIZERSTEP}(\Theta)$  {Apply gradients computed in the loop}

```

C. KG statistics

In Table 4, we show the statistics of all six KGs we use with number of entities, relations, training, validation and test edges. For ATLAS-Wiki-Triple-Sample, we construct a 6.4% subgraph from ATLAS-Wiki-Triple using degree-weighted edge sampling. Edge sampling probability is proportional to the sum of endpoint node degrees, prioritizing connections between high-degree (hub) nodes to preserve the graph’s core topological structure.

Table 4. KG statistics with number of entities, relations, training, validation and test edges.

Dataset	Entities	Relations	Train Edges	Valid Edges	Test Edges	Total Edges
FB15k	14,951	1,345	483,142	50,000	59,071	592,213
FB15k-237	14,505	237	272,115	17,526	20,438	310,079
NELL995	63,361	200	114,213	14,324	14,267	142,804
FB400k	409,829	918	1,075,837	537,917	537,917	2,151,671
ogbl-wikikg2	2,500,604	535	16,109,182	429,456	598,543	17,137,181
ATLAS-Wiki-Triple-4M	4,035,238	512,064	23,040,868	2,880,108	2,880,110	28,801,086

D. Implementation Details

Asynchronous Parallelism and Pipelining. We implement a decoupled execution pipeline characterized by two key parallelization strategies:

- **Multi-stream Operator Execution:** We leverage independent CUDA streams to parallelize disjoint operator types within the QueryDAG. This allows for the simultaneous execution of compute-bound and memory-bound kernels, effectively masking hardware latency.
- **Heterogeneous Pipelining:** To mitigate the bottleneck of CPU-side data preparation, we introduce a consumer-producer pipeline. While the GPU executes current operator batches, the CPU concurrently performs asynchronous sampling for subsequent queries, ensuring a continuous data flow to the accelerators.

Hyperparameters and Configuration. Table 5 summarizes the unified hyperparameter settings applied across all baseline query encoding models and the configuration for the Qwen3 semantic integration. To ensure a fair comparison with prior work, we maintain a consistent training environment: all baselines are initialized with a latent dimension of 400 and trained using the same negative sampling strategy and optimizer configurations.

E. Joint Structural-Semantic Representation

We formalize the integration of semantic information not as a mere feature augmentation, but as a mapping into a **composite representation manifold** $\mathcal{H}_{\text{joint}}$. Specifically, we define the problem as finding a joint embedding for each entity $e_i \in \mathcal{E}$ that simultaneously inhabits two distinct latent subspaces.

Subspace Definitions. The representation space is decomposed into:

1. **Structural Subspace** ($\mathcal{H}_{\text{str}} \in \mathbb{R}^{d_s}$): An endogenous, learnable space optimized to satisfy the relational constraints and multi-hop logical dependencies inherent in \mathcal{G} .
2. **Semantic Subspace** ($\mathcal{H}_{\text{sem}} \in \mathbb{R}^{d_m}$): An exogenous, fixed manifold derived from a pre-trained linguistic encoder $\Phi : \mathcal{D} \rightarrow \mathcal{H}_{\text{sem}}$. For each entity e_i , its semantic prior $\mathbf{z}_i = \Phi(d_i)$ is grounded in its textual description $d_i \in \mathcal{D}$.

Problem Definition: Semantic Grounding. We posit that the complete representation of an entity e_i is a function Ψ that maps the Cartesian product of the two subspaces into the final embedding \mathbf{x}_i :

$$\mathbf{x}_i = \Psi(\mathbf{h}_i, \mathbf{z}_i), \quad \text{s.t. } \mathbf{h}_i \in \mathcal{H}_{\text{str}}, \mathbf{z}_i \in \mathcal{H}_{\text{sem}} \quad (13)$$

where \mathbf{h}_i is a set of adaptive parameters and \mathbf{z}_i acts as an invariant semantic anchor.

Table 5. Hyperparameter settings and model configurations.

Parameter	Value
Batch Size	512 queries
Optimizer	Adam (lr 10^{-4})
Margin (γ)	12.0

Sufficient Statistics for Probabilistic Reasoning. For reasoning frameworks that model queries as probability distributions (e.g., box or beta-based distributions), the task is to define a density function $p(x|\theta_i)$. Under our joint formulation, the parameters θ_i (e.g., location and uncertainty measures) are defined as functionals of the joint space:

$$\theta_i \propto \mathcal{F}(\mathbf{x}_i) = \mathcal{F}(\Psi(\mathbf{h}_i, \mathbf{z}_i)) \quad (14)$$

This formulation ensures that the resulting geometric shapes or distributions in the embedding space are intrinsically constrained by the linguistic grounding of the entities, even when the graph topology is sparse.

F. Stochastic Online Query Sampling

To handle the combinatorial explosion of query structures in Large-scale Knowledge Graphs (KGs), we implement an **Online Stochastic Sampler** \mathcal{S} . Unlike traditional offline methods that rely on pre-computed static datasets, our approach synthesizes training samples *on-the-fly*, ensuring a more comprehensive exploration of the underlying graph distribution.

F.1. Formal Definition and Motivation

Let $\mathcal{G} = (\mathcal{V}, \mathcal{R})$ denote the knowledge graph. A query q can be framed as a subgraph retrieval task. We define the sampling process at training step t as a stochastic mapping:

$$\mathcal{B}_t = \{q_i\}_{i=1}^{|\mathcal{B}|} \sim \mathcal{S}(\mathcal{G}, \mathcal{T}; \pi) \quad (15)$$

where \mathcal{T} represents the set of logical templates and π is the sampling distribution (e.g., uniform or frequency-weighted). The primary motivation for online sampling is to overcome the *data rigidity* of static benchmarks, allowing the model to encounter a near-infinite variety of query-answer pairs (q, \mathcal{A}_q) across the entire training manifold.

F.2. Sampling Strategy and Efficiency

The sampler employs a hybrid strategy to ensure both efficiency and biological/logical plausibility of the generated queries:

- **Dynamic Traversal:** For each batch, the sampler performs a restricted random walk or neighborhood expansion on \mathcal{G} to instantiate logical variables.
- **Constraint Satisfaction:** To maintain query quality, we incorporate a *Rejection Sampling* mechanism. A candidate query q is accepted if it satisfies the structural constraint τ , i.e., $P_{\text{accept}}(q) \propto \mathbb{I}(q \in \mathcal{Q}_{\text{valid}})$, where $\mathcal{Q}_{\text{valid}}$ is the space of queries with non-empty answer sets.
- **Computational Complexity:** By delegating intensive graph traversal to highly optimized low-level primitives (implemented in C++ for parallelism), the sampler achieves a temporal complexity of $\mathcal{O}(k \cdot |\mathcal{B}|)$ per batch, where k is the maximum query depth. This decoupling of data generation from GPU computation ensures that the training throughput is constrained only by model backpropagation, not by I/O bottlenecks.

F.3. Advantages of Online Synthesis

Compared to pre-computation, the online sampler provides three core methodological benefits: 1. **Diversity Maximization:** The probability of the model encountering the exact same query instance twice is $P \approx 0$, which acts as a strong regularizer and prevents overfitting to specific graph patterns. 2. **Zero Storage Overhead:** The spatial complexity for data maintenance is reduced from $\mathcal{O}(|\mathcal{Q}|)$ to $\mathcal{O}(|\mathcal{G}|)$, where $|\mathcal{Q}| \gg |\mathcal{G}|$. 3. **Adaptive Distribution:** The sampling distribution π can be dynamically adjusted during training (e.g., via curriculum learning) to focus on harder reasoning paths without re-generating the dataset.

Table 6. Comparison of execution time per operator: Baseline vs. Batched.

Operator	Baseline (ms)	Batched (ms)	Speedup
EmbedE	2.3	0.8	2.88×
Project	15.7	4.2	3.74×
Intersect	78.5	6.0	13.11×
Union	62.3	5.1	12.22×

F.4. Ablation Speedup Study.

Table 6 isolates the performance gains for specific logical operators. The most dramatic improvements are observed in `Intersect` and `Union` operations ($> 12\times$). These gains are attributed to the high arithmetic intensity and multi-input structure of these operators, which allow the batched execution to saturate GPU compute cores more effectively than memory-bound operations such as `EmbedE`. Furthermore, the attention mechanisms inherent in these compositional operators benefit significantly from the reduced fragmentation provided by batching.

Table 7. Performance (%) of BetaE on queries with negation.

Dataset	Metrics	2in	3in	inp	pin	pni	avg
FB15k	MRR	13.00	14.97	9.17	6.11	11.88	11.03
	Hit@10	26.36	30.56	18.53	11.97	23.74	22.23
FB15k-237	MRR	3.96	6.95	6.52	3.97	2.96	4.87
	Hit@10	7.75	14.19	13.45	7.45	5.08	9.584
NELL995	MRR	4.06	6.65	8.03	3.25	2.92	4.98
	Hit@10	7.84	14.88	16.05	5.61	5.31	9.94
OGB	MRR	36.38	50.92	39.07	39.31	38.50	40.84
	Hit@10	56.24	68.48	57.93	58.63	57.82	59.82

F.5. Performance comparison with and without Semantic Entity Representations

Table 8 presents a quantitative ablation study of the proposed decoupled semantic integration strategy. 1. Throughput Enhancement: By decoupling the computationally intensive Pre-trained Text Encoders (Qwen/BGE) from the online training loop, we achieve a substantial speedup (averaging from 347 to 1915 queries/sec). This validates that our GPU-Resident caching mechanism effectively mitigates the I/O and computational latencies associated with online encoding. 2. Memory Optimization: Notably, our method reduces peak GPU memory usage despite incorporating high-dimensional semantic features. This reduction is attributed to the offloading of large transformer weights post-pre-computation, retaining only the essential embedding buffers in HBM. 3. Predictive Gains: The integration of linguistic priors consistently improves MRR (Average +4.74%), proving particularly effective in sparse data regimes where structural signals are limited.

Table 8. Performance comparison with and without Semantic Entity Representations optimizations across three datasets (FB15k, FB15k-237, NELL995) and three models (BetaE, Q2B, GQE). Solid bars show baseline performance, hatched bars (//) show optimized performance. Higher is better for MRR and throughput; lower is better for memory. The optimizations consistently improve MRR across all models and datasets, dramatically increase training throughput, and modestly reduce memory consumption.

Dataset	Model	MRR (%)		Training queries (Queries/Sec)		GPU Memory (GB)	
		NGDB-Zoo	NGDB-Zoo + Optimizations	NGDB-Zoo	NGDB-Zoo + Optimizations	NGDB-Zoo	NGDB-Zoo + Optimizations
FB15k	BetaE +Qwen-EMB	42.04	46.92	209	1516	14.23	13.11
	Q2B +Qwen-EMB	41.85	50.86	348	2014	6.39	5.18
	GQE +Qwen-EMB	29.39	35.91	558	2254	12.61	11.49
	BetaE +BGE-Base-En-v1.5	42.04	45.37	187	1402	14.40	13.21
	Q2B +BGE-Base-En-v1.5	41.85	47.54	340	1886	6.55	5.23
	GQE +BGE-Base-En-v1.5	29.39	30.17	550	2302	12.74	11.52
FB15k-237	BetaE +Qwen-EMB	21.11	26.03	215	1581	11.14	9.95
	Q2B +Qwen-EMB	20.19	29.54	358	1911	7.34	5.29
	GQE +Qwen-EMB	16.42	22.32	604	2729	10.97	9.89
	BetaE +BGE-Base-En-v1.5	21.11	24.81	200	1503	11.28	10.01
	Q2B +BGE-Base-En-v1.5	20.19	25.72	312	1750	7.46	5.21
	GQE +BGE-Base-En-v1.5	16.42	22.13	534	2401	11.00	9.84
NELL995	BetaE +Qwen-EMB	24.7	27.41	154	1487	8.04	7.11
	Q2B +Qwen-EMB	22.79	26.75	251	2114	6.50	5.44
	GQE +Qwen-EMB	18.4	22.64	538	2698	8.62	7.42
	BetaE +BGE-Base-En-v1.5	24.7	26.41	140	1323	8.16	7.14
	Q2B +BGE-Base-En-v1.5	22.79	26.20	238	1402	6.70	5.54
	GQE +BGE-Base-En-v1.5	18.4	22.37	515	2201	8.75	7.48
Average		26.32	31.06	347	1915	9.60	8.34